International Journal of Electrical, Electronic and Communication Sciences
ISSN: 2517-9438
Vol:12, No:3, 2018

Cavity-Type Periodically-Poled $LiNbO_3$ Device for Highly-Efficient Third-Harmonic Generation

Isao Tomita

***Abstract*—**We develop a periodically-poled $LiNbO_3$ (PPLN) device for highly-efficient third-harmonic generation (THG), where the THG efficiency is enhanced with a cavity. THG can usually be produced via $\chi^{(3)}$-nonlinear materials by optical pumping with very high pump-power. Instead, we here propose THG by moderate-power pumping through a specially-designed PPLN device containing only $\chi^{(2)}$-nonlinearity, where sum-frequency generation in the $\chi^{(2)}$ process is employed for the mixing of a pump beam and a second-harmonic-generation (SHG) beam produced from the pump beam. The cavity is designed to increase the SHG power with dichroic mirrors attached to both ends of the device that perfectly reflect the SHG beam back to the device and yet let the pump and THG beams pass through the mirrors. This brings about a THG-power enhancement because of THG power proportional to the enhanced SHG power. We examine the THG-efficiency dependence on the mirror reflectance and show that very high THG-efficiency is obtained at moderate pump-power when compared with that of a cavity-free PPLN device.

***Keywords*—**Cavity, periodically-poled $LiNbO_3$, sum-frequency generation, third-harmonic generation.

I. Introduction

MUCH focus is now being placed on highly-efficient third-harmonic generation (THG) in scientific and technological studies, including studies on the determination of absolute frequencies in an optical comb (i.e., ultra-precisely arranged spectral lines with an equal spacing). This optical comb has photonic high-tech applications, such as precise measurements of atomic absorption spectral lines [1] and wavelength-division-multiplexing (WDM) optical communications [2]. Two researchers who developed the optical-comb generation (together with a self-referencing technique [3], [4] by use of second-harmonic generation (SHG)) were awarded Nobel prize in physics in 2005 [5], and the research in this field has been propelled worldwide. In the application to WDM communications, the optical comb is used as optical broadband frequencies that enable huge data-throughput in our optical networks and thus enrich our daily lives with smooth digital optical communications. In addition, the development of high-power, compact green lasers (e.g., at 520 nm) with THG is now drawing much attention towards various laser applications, including full-color, high-resolution laser projectors. Thus, highly-efficient THG is in great demand.

Isao Tomita is with Department of Electrical and Computer Engineering, National Institute of Technology, Gifu College, 2236-2 Kamimakuwa, Motosu, Gifu 501-0495, Japan (e-mail: itomita@gifu-nct.ac.jp) and also with School of Electronics and Computer Science, University of Southampton, SO17 1BJ, UK.

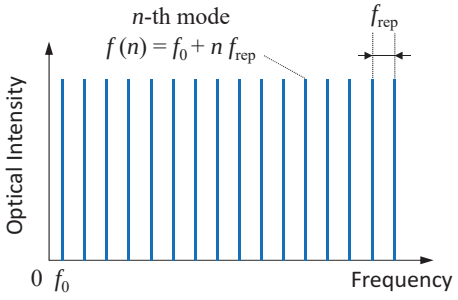

Fig. 1 Optical frequencies in the optical comb. If f_0 is measured very precisely, then all the frequencies are perfectly determined

II. Usage of THG

As an example of the usage of THG, we show how to use it to determine the absolute frequencies of a beam generated from a mode-locked laser (i.e., a pulse laser) and a photonic-crystal fiber [6]. In this case, the n-th mode $f(n)$ of the frequencies is given by

$$f(n) = f_0 + nf_{\rm rep}, \tag{1}$$

where f_0 is an offset frequency ($0 \leq f_0 < f_{\rm rep}$), which is unknown when the beam is generated, n is an integer (including 0), and $f_{\rm rep}$ is a repetition frequency of the optical pulses, which is known in advance with a very high precision of $\Delta f/f_{\rm rep} < 3 \times 10^{-17}$ [7], where Δf is a frequency shift from $f_{\rm rep}$ in the mode spacing of the optical comb.

If the unknown f_0 is determined with very high accuracy, all the frequencies are perfectly determined, and the optical comb can be used as *a precise frequency scale*.

To obtain f_0, we use THG in the following way: First, we produce THG of frequency $3f(n)$ through a $\chi^{(3)}$ material (e.g., Si [8]) and SHG of frequency $2f(m)$ through a $\chi^{(2)}$ material (e.g., $LiNbO_3$ [9]) from a beam of frequency $f(n)$. In this case, $3f(n)$ and $2f(m)$ are of the form:

$$3f(n) = 3f_0 + 3nf_{\rm rep}, \tag{2}$$
$$2f(m) = 2f_0 + 2mf_{\rm rep}. \tag{3}$$

We then extract a beat frequency $f_{\rm beat}$ via optical heterodyne detection from a beat between the $3f(n)$- and $2f(m)$-beams for the modes that suffice $3n = 2m$, i.e.,

$$f_{\rm beat} = 3f(n) - 2f(m) = f_0. \tag{4}$$

Here, the issue on THG in the above scheme is that the THG power (obtained with Si) is rather small compared with the SHG power (obtained with $LiNbO_3$). The enhancement

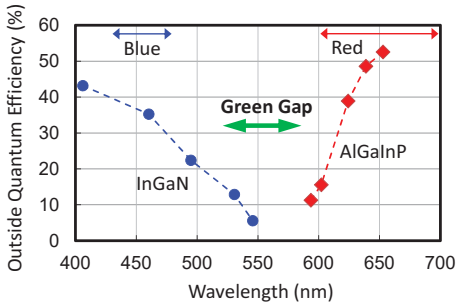

Fig. 2 Outside quantum efficiency vs wavelength in semiconductor LDs. There is a region called a green gap at around 550 nm, where the outside quantum efficiency is very low

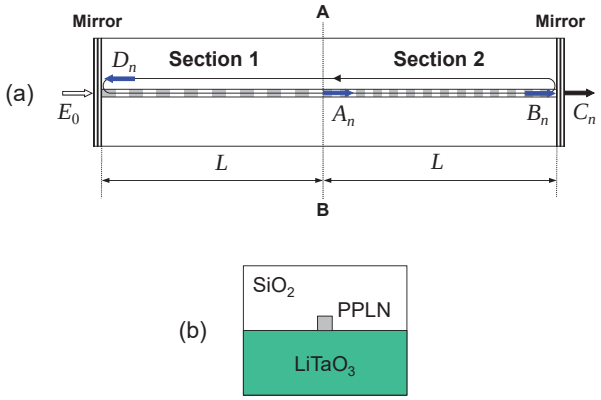

Fig. 3 Proposed device structure with a cavity, where the cavity is formed with dichroic mirrors attached at both ends of the device. (a) Top view of the device. (b) Cross-sectional view of the device at a plane that contains points A and B in (a)

of THG power makes the beat-frequency measurement much easier.

The second example is a green-laser application. So far, high-power red and blue laser diodes (LDs) have been successfully developed along with their good semiconductor-crystal growth by metal organic chemical vapor deposition (MOCVD). But, green LDs are still developing because a quality improvement in their crystal growth is underway. Within the conventional techniques and crystal-growth conditions, very small outside quantum efficiency was achieved for green LDs at a wavelength of around 550 nm, as shown in Fig. 2 [10]. This low-efficiency region is called *a green gap*. Fortunately, Yanashima et al. have recently developed new green LD structures while using epitaxial growth for InGaN and have succeeded in fabricating green LDs with an output power of 50-70 mW [11].

However, since the above LDs fabricated with some special techniques and structures are costly and have a finite lifetime (or a finite time-period where constant output power is obtained), we employ another method to generate green beams with THG by use of an inexpensive periodically-poled $LiNbO_3$ (PPLN) and a commercially available 1.56-μm LDs for wide industrial applications that require stable, long-lifetime operations. This type of PPLN has been developed until now [14], but its output efficiency is rather low. The device structure proposed in the present paper can overcome this low efficiency.

In the next section, we show our device structure that employs a cavity of dichroic mirrors to boost the efficiency.

III. Device Structure and Function

The device structure for green-THG using PPLN with a cavity is illustrated in Fig. 3. Fig. 3 (a) is a top view of the PPLN device, which has dichroic mirrors (dielectric multilayer mirrors) at both ends of the device as the cavity. The cavity enhances the SHG power inside the device, where the mirrors reflect only the SHG beam and let the pump and THG beams pass through the mirrors via the adjustment of the dielectric multilayer periods. This cavity gives rise to a THG-power enhancement owing to the THG power proportional to the enhanced SHG power.

Fig. 3 (b) is the device cross-sectional view at a plane that contains points A and B shown in Fig. 3 (a). The PPLN waveguide in Fig. 3 (b) is formed on a $LiTaO_3$ substrate with a smaller refractive index ($n_{LiTaO_3} = 2.17$) than that of the PPLN waveguide ($n_{LiNbO_3} = 2.21$), thereby confining propagating beams to the PPLN waveguide. The upper region of the PPLN waveguide is covered with sputtered SiO_2 ($n_{SiO_2} = 1.45$) to protect the waveguide, where there is a merit that this makes the fabrication of the mirrors easier at the waveguide ends, because the ends can have a wide area after burial of the waveguide in the SiO_2/$LiTaO_3$-sandwiched structure.

In Fig. 3 (a), SHG is performed at Section I from a pump beam coming from the left (i.e., outside the device), where the period of the periodic poling is set so that the pump-beam frequency f_0 is converted to an SHG frequency $f_{SHG} = 2f_0$ [12], [13]. At Section II, sum-frequency generation (SFG) is performed by the frequency mixing of the pump and SHG beams, which gives the output frequency $f_{output} = f_{SHG} + f_0 = 3f_0 (= f_{THG})$, where the PPLN poling period is set so as to give $f_{output} = f_{SHG} + f_0 = 3f_0$. As a numerical example for the output frequency (wavelength), if we use the pump frequency (wavelength) at $f_0 = 192.1$ THz (1.56 μm), then we can obtain $f_{THG} = 576.5$ THz (0.52 μm) as the THG frequency (wavelength).

The next section provides THG-power analysis in the above scheme using SHG and SFG.

IV. THG-Power Analysis

A. Computational Method

We assume that the mirrors in Fig. 3 (a) have a reflection amplitude r for the SHG beam that travels from the inside to the outside of the device. This r has a relation with the transmission amplitude t as $r^2 + t^2 = 1$ (r, t: real numbers). The total length of the PPLN waveguide is set to be $2L$, where the waveguide for both SHG (Section I) and SFG (Section II) has the same length L. The mirrors reflect the SHG beam back to the device with a reflectance of r^2, and SHG photons are accumulated inside the device. The enlarged SHG power (P_{SHG}) inside the device increases the output THG power

($P_{\rm THG}$) because THG caused by SFG between the pump and SHG beams gives a power of $P_{\rm THG} \propto P_0\, P_{\rm SHG}$, where P_0 is the pump power, which is a constant. Note that the phase shifts at reflection at the device ends are adjusted by refractive-index control of the device with such a temperature controller as a Peltier device. If there is another phase shift (due to another physical mechanism), it can also be removed by the refractive-index control.

In Fig. 3 (a), we set E_0 and θ to be the electric-field amplitude of the pump beam and the phase shift of the SHG beam at reflection with the mirrors, respectively. We then have the following recurrence equations for the SHG electric-field amplitudes:

$$A_n = \kappa_{\rm SHG}\,|E_0|^2 + r\,e^{i\theta}\,D_{n-1}\,e^{-\alpha L/2}, \quad (5)$$
$$B_n = A_n\,e^{-\alpha L/2}, \quad (6)$$
$$C_n = \kappa_{\rm SFG}\,E_0\,A_n\,e^{-\alpha L/2}, \quad (7)$$
$$D_n = r\,e^{i\theta}\,B_n\,e^{-\alpha L}, \quad (8)$$

where A_n is the amplitude of the right-going SHG beam at the halfway point, B_n is that of the right-going SHG beam at the rightmost point, C_n is that of the SFG beam going outside the device, D_n is that of the left-going SHG beam at the leftmost point, n represents the beam circulation number, α is the beam propagation loss, and $\kappa_{\rm SHG,SFG}$ is a factor related to the SHG-, SFG-efficiency coefficient $\eta_{\rm SHG,SFG}$ as $\eta_{\rm SHG,SFG} = \kappa^2_{\rm SHG,SFG}/S$ with S being the waveguide cross-sectional area. In the above, no-pump-depletion approximation [9] that ignores the power attenuation of $|E_0|^2$ was employed, using very large $|E_0|$ compared with $|A_n|, |B_n|, |C_n|, |D_n|$. Yet, the power attenuation of these small amplitudes $|A_n|, |B_n|, |C_n|, |D_n|$ was taken into account, because the total path for them with n-th circulation will be far longer (at $n \to \infty$) than that of the pump beam with E_0 passing through the device only once.

In (5)-(8), the initial conditions (i.e., $n = 1$) are set as

$$A_1 = \kappa_{\rm SHG}\,|E_0|^2, \quad (9)$$
$$B_1 = A_1 e^{-\alpha L/2}, \quad (10)$$
$$C_1 = \kappa_{\rm SFG}\,E_0\,A_1\,e^{-\alpha L/2}, \quad (11)$$
$$D_1 = r\,e^{i\theta}\,B_1\,e^{-\alpha L}. \quad (12)$$

With the conditions (9)-(12), by solving (5)-(8) and setting $n \to \infty$, we obtain the THG intensity as

$$|E_{\rm THG}|^2 = |C_\infty|^2 = \kappa^2_{\rm SFG}\kappa^2_{\rm SHG}\,|E_0|^6\,e^{-\alpha L}\,\Gamma, \quad (13)$$

where

$$\Gamma = \frac{1}{1 - 2r^2 e^{-2\alpha L}\cos 2\theta + r^4 e^{-4\alpha L}} \quad (14)$$

is a THG enhancement factor, where $\Gamma = 1$ corresponds to the no-cavity case. If we convert $|E_{\rm THG}|^2$ in (13) in units of W/m^2 to a power $P_{\rm THG}$ in units of W (where $|E_{\rm THG}|^2$ was already converted to an optical intensity by the multiplication of a factor $\sqrt{\epsilon_0 nc/2}$ (ϵ_0: vacuum permittivity, n; waveguide refractive-index, c: light velocity)), we should multiply $|E_{\rm THG}|^2$ by S (i.e., $P_{\rm THG} = S|E_{\rm THG}|^2$), where S is typically (3 μm)^2. In this case, $P_{\rm THG}$ is of the form.

$$P_{\rm THG} = \eta_{\rm SFG}\eta_{\rm SHG}P_0^3\,e^{-\alpha L}\,\Gamma \quad (15)$$
$$= 2\eta^2_{\rm SHG}P_0^3\,e^{-\alpha L}\,\Gamma, \quad (16)$$

where $\eta_{\rm SFG}$ is the SFG-efficiency coefficient that is related to the SHG-efficiency coefficient $\eta_{\rm SHG}$ as $\eta_{\rm SFG} = 2\eta_{\rm SHG}$, which is obtained from $\eta_{\rm SHG} \propto f_0^2$ and $\eta_{\rm SFG} \propto f_0 f_{\rm SHG} = 2f_0^2$ [15]. THG efficiency defined as $\mathcal{T} = P_{\rm THG}/P_0$ is then given by

$$\mathcal{T} = 2\eta^2_{\rm SHG}P_0^2\,e^{-\alpha L}\,\Gamma, \quad (17)$$

which also increases with increasing Γ.

The next subsection provides numerical results on the enhancement factor Γ and the enhanced power $P_{\rm THG}$ using realistic device parameters.

B. Numerical Results and Discussion

In this subsection, Γ is first computed with experimental values of $L = 3.0$ mm and $\alpha = 0.253$/cm (1.1 dB/cm) [16]. Here, the phase shift 2θ is set to be $2\pi l$ (l is an integer) by the refractive-index adjustment via temperature control. In this case, the dependence of Γ on the mirror reflectance r^2 is shown in Fig. 4 by the blue curve. In Fig. 4, we observe that Γ becomes large monotonically as r^2 increases via steady accumulation of SHG photons. At $r^2 = 1$ (i.e., 100% reflectance), $\Gamma = 50.3$ is obtained; that is, $P_{\rm THG}$ at $r^2 = 1$ is 50.3 times greater than that without the cavity (i.e., at $r^2 = 0$). Since the value of Γ at around $r^2 = 0$ (in the no-cavity case) is not clearly seen in Fig. 4, a figure with the logarithmic plot of the vertical axis is given in the inset of Fig. 4, where we can see that Γ actually starts from 1 at $r^2 = 0$.

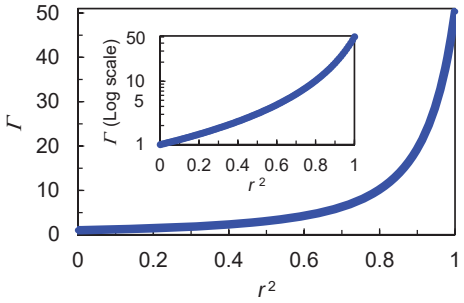

Fig. 4 Mirror reflectance r^2 dependence of the THG enhancement factor Γ. The inset shows a figure with the logarithmic scale of the vertical axis

We then calculate the size of $P_{\rm THG}$ at $r^2 = 1$ by use of $\eta_{\rm SHG} \approx 50$ %/W [16] at $P_0 = 100$ mW, and obtain $P_{\rm THG} \approx 23.3$ mW (i.e., $\mathcal{T} \approx 23.3$ %) by the cavity effect. For a comparison, we show $P_{\rm THG}$ at $r^2 = 0$ (i.e., without the cavity): $P_{\rm THG} \approx 0.46$ mW (i.e., $\mathcal{T} \approx 0.46$ %). In this THG-power enhancement, very large SHG power has been achieved at $r^2 = 1$, which could cause THG power instability via a phase shift due to the large SHG power density. Since this cannot be avoided in principle, an appropriate setting of r^2 (which should be set less than 1 while keeping Γ large) [17] will be necessary in practical use of the proposed method; even in this case, several tens of Γ will be obtained.

V. Summary

We have analyzed THG power P_{THG} and its enhancement factor Γ in a cavity-type PPLN device that makes possible highly-efficient THG, where THG is performed by SFG between a pump beam and a SHG beam produced by the frequency-doubling of the pump beam. The proposed device design with a cavity composed of dichroic mirrors has had a function that the mirrors perfectly reflect the SHG beam back to the device and let the pump and THG beams pass through the mirrors. This has given rise to a THG-power enhancement because the THG power is in proportion to the increased SHG power. By analyzing the THG-efficiency dependence on the mirror reflectance r^2, we have demonstrated that very high THG efficiency can be achieved near $r^2 = 1$ when compared with that of a cavity-free PPLN device (i.e., with $r^2 = 0$). The proposed device has various photonic high-tech applications, including the absolute-frequency determination of the optical comb and the full-color, high-resolution laser projectors that guarantee stable, long-lifetime operations.

Acknowledgment

The author would like to thank Ogawa Science & Technology Foundation for the financial support to attend the ICECE2018 conference and to publish this paper.

References

[1] Th. Udem, J. Reichert, R. Holzwarth, and T. W. Hänsch, "Absolute optical frequency measurement of the cesium D_1 line with a mode-locked laser," Phys. Rev. Lett. 82, 1999, pp.3568-3571.
[2] K. Mori and K. Sato, "Supercontinuum lightwave generation employing a mode-locked laser diode with injection locking for a highly coherent optical multicarrier source," IEEE Photon. Tech. Lett. 17, 2005, pp.480-482.
[3] D. J. Jones, S. A. Diddams, J. K. Ranka, A. Stentz, R. S. Windeler, J. L. Hall, S. T. Cundiff, "Carrier-envelope phase control of femtosecond mode-locked lasers and direct optical frequency synthesis," Science 28, 2000, pp.635-640.
[4] K. Sugiyama, "Optical frequency measurement with mode-locked lasers," Optics (Opt. Soc. Jpn) 31, 2002, pp.870-876.
[5] J. L. Hall and T. W. Hänsch, "For their contributions to the development of laser-based precision spectroscopy, including the optical frequency comb technique," Nobel Prize in Physics, 2005. https://www.nobelprize.org.
[6] P. Russell, "Photonic crystal fibers," Science 17, 2003, pp.358-362.
[7] Th. Udem, J. Reichert, R. Holzwarth, and T. W. Hänsch, "Accurate measurement of large optical frequency differences with a mode-locked laser," Opt. Lett. 24, 1999, pp.881-883.
[8] M. Mehendale, S. A. Mitchell, J. P. Likforman, D. M. Villeneuve, and P. B. Corkum, "Method for single-shot measurement of the carrier envelope phase of a few-cycle laser pulse," Opt. Lett. 25, 2000, pp.1672-1674.
[9] A. Yariv, *Optical Electronics in Modern Communications*, 5th ed. (Oxford University Press, Oxford, 1997).
[10] T. Nakamura, "Development of the world's first true green laser diodes," Production & Technology 65, 2013, pp.79-81.
[11] K. Yanashima, H. Nakajima, K. Tasai, K. Naganuma, N. Fuutagawa, Y. Takiguchi, T. Hamaguchi, M. Ikeda, Y. Enya, S. Takagi, "Long-lifetime true green laser diodes with output power over 50 mW above 525 nm grown on semipolar $\{20\bar{2}1\}$ GaN substrates," Appl. Phys. Exp. 5, 2012, 082103 (3 pages).
[12] J. A. Armstrong, N. Bloembergen, J. Ducuing, and P. S. Pershan, "Interactions between light waves in a nonlinear dielectric," Phys. Rev. 127, 1962, pp.1918-1939.
[13] M. M. Fejer, G. A. Magel, D. H. Jundt, and R. L. Byer, "Quasi-phase-matched second harmonic generation: tuning and tolerances," IEEE J. Quantum. Elec. 28, 1992, pp.2631-2654.
[14] K. Kintaka, M. Fujimura, T. Suhara, and H. Nishihara, "Third harmonic generation of Nd:YAG laser light in periodically poled $LiNbO_3$," Elec. Lett. 33, 1997, pp.1459-1461.
[15] R. W. Boyd, *Nonlinear Optics*, 1st ed. (Academic Press, San Diego, 1992).
[16] M. Fujimura, M. Sudoh, K. Kintaka, T. Suhara, H. Nishihara, "Enhancement of SHG efficiency in periodically poled $LiNbO_3$ waveguide utilising a resonance effect," Electron. Lett. 32, 1996, pp.1283-1284.
[17] I. Tomita, "Highly-efficient cascaded difference-frequency generation in periodically-poled $LiNbO_3$ devices with resonators," IEEJ Trans. Electrical and Electronic Eng. 2017 (Accepted). A similar output instability occurs in [17] as long as a similar cavity structure for SHG beams is employed, where the enhancement factor β in [17] is almost the same form as Γ obtained in the present paper.